Plasma-Chemical Disposal of Silicon and Germanium Tetrachlorides Waste by Hydrogen Reduction

Roman Kornev , Igor Gornushkin , Lubov Shabarova , Alena Kadomtseva , Georgiy Mochalov * , Nikita Rekunov , Sergey Romanov , Vitaly Medov , Darya Belousova , Nikita Maleev

Posted Date: 9 November 2023

doi: 10.20944/preprints202311.0611.v1

Keywords: high-frequency arc discharge; hydrogen reduction; silicon chlorides; germanium chlorides

Article

Plasma-Chemical Disposal of Silicon and Germanium Tetrachlorides Waste by Hydrogen Reduction

Roman Kornev [1,3], Igor Gornushkin [5], Lubov Shabarova [1,4], Alena Kadomtseva [2], Georgyi Mochalov [3,*], Nikita Rekunov [3], Sergey Romanov [3], Vitaly Medov [3], Darya Belousova [3] and Nikita Maleev [3]

[1] Institute of Chemistry and High-Purity Substances of the Russian Academy of Sciences named after G.G. Devyatykh, Tropinina, 49, Nizhny Novgorod, Russia 603951; romanakornev@gmail.com
[2] Privolzhsky Research Medical University, Minina and Pozharskogo Square 10/1, Nizhny Novgorod, Russia 603005
[3] R.E. Alekseev Nizhny Novgorod Technical University, Minin St., 24, Nizhny Novgorod, Russia 603155; biotehno@nntu.ru
[4] National Research Lobachevsky State University of Nizhny Novgorod, Prospekt Gagarina 23, Nizhny Novgorod, Russia 603022
[5] BAM Federal Institute for Materials Research and Testing, Richard-Willstätter-Strasse 11, Berlin, Germany 12489
* Correspondence: e.mochalo@gmail.com

Abstract: The processes of hydrogen reduction of silicon and germanium chlorides under the conditions of high-frequency (40.68 MHz) counteracted arc discharge stabilized between two rod electrodes are investigated. The main gas-phase and solid products of plasma-chemical transformations are determined. Thermodynamic analysis of $SiCl_4$ + H_2 and $GeCl_4$ + H_2 systems for optimal process parameters was carried out. Using the example of hydrogen reduction of $SiCl_4$ by the method of numerical modeling, gas-dynamic and thermal processes for this type of discharge are investigated. The impurity composition of gas-phase and solid reaction products is investigated. The possibility of single-stage production of high-purity Si and Ge mainly in the form of compact ingots, as well as high-purity chlorosilanes and trichlorogermane, is shown.

Keywords: high-frequency arc discharge; hydrogen reduction; silicon chlorides; germanium chlorides

1. Introduction

Silicon and germanium are the most popular materials for microelectronics [1], photovoltaics [2–5], infrared optics [6–8], as well as for development of ionizing radiation detectors [9,10]. Modern technology for obtaining these materials is based on the processes of processing their high-purity chlorides and hydrides [11–13].

Virtually all silane used in hydride technology is obtained by the catalytic dismutation reaction of trichlorosilane (TCS) [14,15]. In this reaction, in addition to silane, a sixteen-fold mass amount of silicon tetrachloride (STC) is obtained, which is subject to disposal.

Another source of STC waste is the Siemens process of producing polysilicon by reducing TCS, where STC is formed as a by-product [1]. In addition, in the process of TCS synthesis, 50–60 mole% of STC are formed by the silicon hydrochlorination reaction as a by-product [16]. In this regard, the utilization of STC by reducing it to TCS or semiconductor silicon will make it possible to organize the production of silicon both using hydride technology and using the Siemens process in a closed and environmentally friendly manner .

For germanium, the source of waste germanium tetrachloride (GTC) is the process of its deep purification by chemical, adsorption, absorption, and distillation methods [17].

The chemical high-temperature method of processing STC into TCS, used in technological schemes for the production of silicon, has a low percentage of TCS output (not more than 20%) and

 doi:10.20944/preprints202311.0611.v1

high energy costs (according to Silicon Products Bitterfeld GmbH & Co. KG, more than 10 kW/h per 1 kg of STC). In this regard, it is promising to develop less energy-consuming methods for converting STC into chlorosilanes and silicon.

From this point of view, it is possible to use plasma-chemical methods for converting STC to chlorosilanes ($SiHCl_3$, SiH_2Cl_2) and silicon.

In order to obtain silicon in the form of bulk samples, in the works [17], the hydrogen reduction process of the STC was carried out under microwave (2.45 GHz) discharge conditions at a pressure of 100 kPa. Agglomerated μ-Si dendritic structures were obtained. However, the samples obtained were powdered silicon, making it difficult to obtain high-purity ingots. In [19], a microwave discharge in a mixture of $SiCl_4$ with H_2 and Ar at a pressure of 26 to 40 kPa was used to obtain $SiHCl_3$. In [20,21], TCS was obtained in an arc, and in [22], in a high-frequency (13.56 MHz) plasmatron. It should be noted that the content of impurities in TCS was at the level of purity of the initial STC. The issue of maintaining the level of purity in the production of silicon in the works [19–22] was not considered.

The production of germanium by the traditional method by hydrolysis of $GeCl_4$ with further reduction of hydrogen oxide is multistage and energy-intensive. In this regard, the reduction of $GeCl_4$ by hydrogen in one stage is attractive. By analogy with STC, with plasma-chemical hydrogen reduction of $GeCl_4$, one can expect the formation of not only germanium, but also chlorogermans of the $GeHnCl_{4-n}$ composition. These compounds are used in pharmacology to develop a variety of biologically active germanium-containing drugs [24,25].

A small number of papers on plasma-chemical hydrogen reduction of $GeCl_4$ are presented in the literature. Nanoparticles of germanium were obtained in the works [26,27] in the annular discharge with capacitive coupling in the $GeCl_4/H_2/Ar$ mixture. In [28], a 300 W HF discharge with a frequency of 13.56 MHz at a pressure of 2.5 Torr was used to obtain chalcogenide films of the GeS_2 composition from a mixture of $GeCl_4$ + H_2S in a $GeCl_4/H_2S$ ratio of 1.5 to 50. In [30]. it is reported that when processing liquid $GeCl_4$ under the conditions of HF pulsed discharge, in the frequency range of 0.001–100 MHz, with a pulse repetition frequency and amplitude of 0.05–50 MHz and 1–8 kV, respectively, Ge_2Cl_6 is formed at atmospheric pressure.

In this regard, the purpose of this study was: 1) an experimental study of the hydrogen reduction processes of STC and $GeCl_4$ under the conditions of high-frequency arc (HFA) discharge, stabilized by two electrodes in a wide range of pressures and reagent ratios and determination of reaction products; 2) thermodynamic analysis of Si/H/Cl and Ge/H/Cl systems, as well as gas-dynamic analysis of processes in the RF-arc discharge plasmatron and comparison, where possible, of the results of calculations with the results of experiments; 3) characterization of the obtained substances.

2. Materials and Methods

2.1. Materials

The following substances were used as starting materials: STC and GTC (99.999%, HORST Ltd., Russia) and hydrogen (99.99998%, Monitoring, Russia). The plasma chemical reactor used W and Si electrodes with a material purity of 99.999% (Sarnia Inc., Russia).

2.2. Experimental conditions

Experiments on the study of the processes of reduction of silicon tetrachloride and germanium in hydrogen plasma were carried out on the installation, the schematic diagram of which is shown in Figure 1. The power of the high-frequency oscillator was 340 W, frequency 40.68 MHz. The flow rate of the plasma-forming gas H_2+$SiCl_4$($GeCl_4$) was varied in the range of 100–700 cm^3/min. The pressure during the experiment was changed in the range of 70–1330 Torr. The molar ratio of $H_2/SiCl_4$($GeCl_4$) was changed in the range of 2–5. The study of the process of plasma-chemical reduction of $SiCl_4$ ($GeCl_4$) in hydrogen plasma of the RF-arc discharge was carried out at a constant energy level of 300 kJ/mol. The value of the energy deposit was determined as the ratio of the power supplied to the gas discharge zone to the flow rate of the plasma-forming gas.

Preprints (www.preprints.org) | NOT PEER-REVIEWED | Posted: 9 November 2023 doi:10.20944/preprints202311.0611.v1

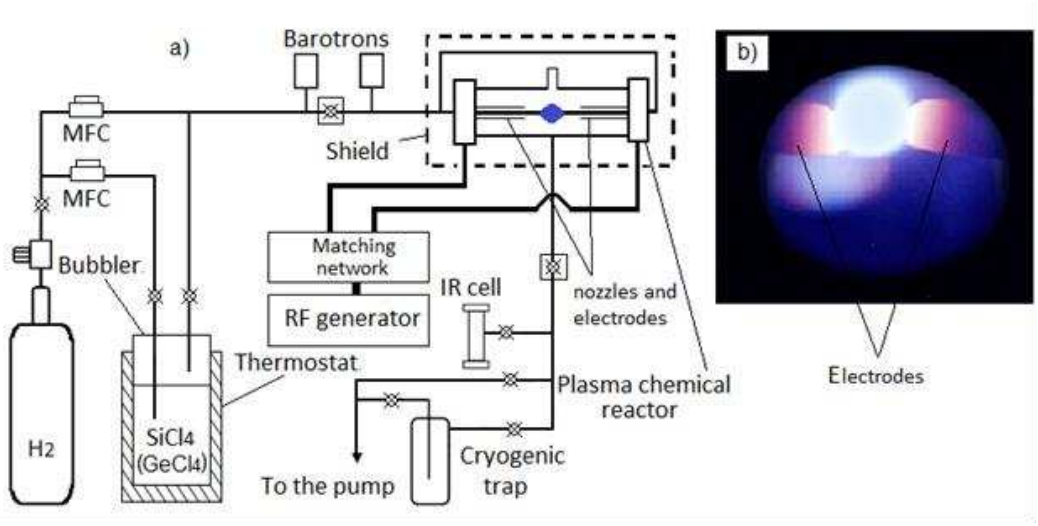

Figure 1. Installation of plasma-chemical reduction of silicon and germanium tetrachlorides in RF-arc discharge (**a**); type of gas discharge in H2+SiCl4 atmosphere at P=760 torr (**b**).

The plasma-chemical reactor was a tube of quartz glass with a diameter of 60 mm with coaxial electrodes. High-frequency voltage was applied to the electrodes from the generator through the matching device and a discharge was ignited between the electrodes. A vapor-gas mixture of STC (GTC) and hydrogen was fed into the discharge volume. The power supplied to the gas discharge zone was determined by the calorimetric method according to the method [30]. When reducing STC, silicon electrodes (Ø 6 mm) were used, and when reducing GTC, tungsten electrodes (Ø 4 mm) were used.

The dependence of the degree of conversion of $SiCl_4$ ($GeCl_4$), the yield of chlorosilanes and chlorogermans, as well as silicon and germanium, on the pressure and molar ratio of reagents was experimentally investigated. The yield of silicon and germanium was determined by the gravimetric method with an accuracy of $1 \cdot 10^{-4}$ g.

The content of chlorosilanes, chlorogermans, and impurities of organic substances in them was determined by gas chromatography using a 3 m long packed column with N-AW-HMDS chromaton (0.16–0.20 mm) with a 15% liquid phase E-301 at a temperature of 373 K, a thermal conductivity detector with a detection limit of 0.008%, or an ionization detector in a flame with a detection limit of 0.00001%, as well as IR spectroscopy of the absorption spectra of reactor gases in the range of 450–7000 cm^{-1} obtained using an IR spectrometer (Bruker Vertex 80v) equipped with a DTGS detector. Resolution and aperture were 1 cm^{-1} and 5 mm, respectively. The gas mixture at the outlet of the reactor was taken into a cuvette with an optical path length of 10 cm. The pressure in the IR cuvette was 50 Torr.

In the study of plasma-chemical reduction of $SiCl_4$ ($GeCl_4$), the content of impurities of metals, electroactive impurities and impurities of organic substances in the initial silicon and germanium chlorides, as well as in the obtained TCS, silicon and germanium by gas chromatography on the Tsvet-800 device, ICP-MS on the ELEMENT-2 device (Thermo Scientific) and atomic emission spectroscopy (AES) on the STE-1 spectrograph was monitored. In the case of nuclear power plants, impurities from volatile chlorides were pre-concentrated by distillation at 0.1 g of the coal sample, and in the case of ICP-MS, impurities were concentrated by distillation on the walls of an optical quartz ampoule, followed by washing them with high-purity nitric acid. The detection limit of the methods was 10^{-7}–10^{-9} wt%.

Morphological studies and analysis of the elemental composition of the samples were carried out using the methods of raster electron microscopy and x-ray microanalysis.

The SEM image of the silicon electrode was obtained using a Tescan Vega II electron microscope at a voltage of 20 kV with a backscattered electron detector (BSE) and a reflected electron detector (RE detector) with a magnification of 500 to 8000 and 20,000. The use of BSE and RE detectors allows for more contrast images compared to the SE detector.

Preprints (www.preprints.org) | NOT PEER-REVIEWED | Posted: 9 November 2023 doi:10.20944/preprints202311.0611.v1

A transmission electron microscope (TEM) JEM 2100, JEOL, Japan, was used for structural studies of the powdered Ge.

2.3. Theoretical part

Calculations of the thermodynamically equilibrium composition were performed using open-source software [31,32] using the algorithm [33,34] corrected in [35] to calculate the equilibrium composition of hydrogen and argon-hydrogen plasma in the presence of silicon and germanium halides.

For the theoretical calculation of the temperature and concentration distribution profile in the plasma-chemical reactor, the method of numerical CFD modeling was used. The calculation was carried out according to the method presented in [36]. Thermophysical and transport characteristics of media are taken from [37].

3. Results

3.1. Hydrogen reduction of $SiCl_4$

The dependence of the degree of conversion of $SiCl_4$ to chlorosilanes and silicon on the ratio of reagents in the initial mixture is shown in Figure 2a. The maximum yield of $SiHCl_3$ (44%) is observed at the ratio $H_2/SiCl_4$=6.9. With a further increase in the concentration of hydrogen, the yield of TCS decreases. The yield of Si with increasing hydrogen concentration monotonically increases from 8 to 47%, and the yield of SiH_2Cl_2 from 3 to 8%. It should be noted that the results for the yield of TCS (Figure 2 a) are in good agreement with the data [40].

Depending on the pressure (Figure 2 b), an extreme TCS yield relationship is observed with a maximum pressure of 550 Torr. With an increase in pressure above 1 atm, an increase in discharge contracting is observed, and at a constant discharge power, the burning stops at a pressure of 1330 Torr (1.75 atm).

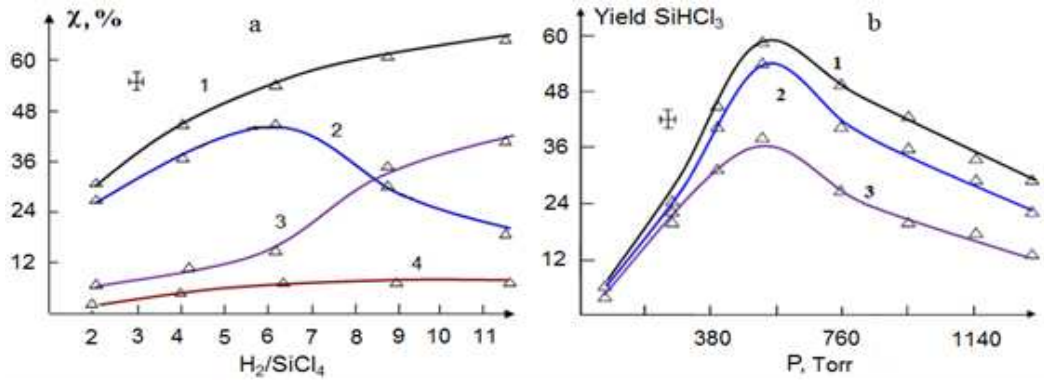

Figure 2. The total degree of conversion of $SiCl_4$ (1), the yield of $SiHCl_3$ (2), Si (3) and SiH_2Cl_2 (4) depending on the ratio of $H_2/SiCl_4$ (**a**); the dependence of the yield of $SiHCl_3$ on the pressure in the reactor at a different ratio of $H_2/SiCl_4$ (**b**); the ratio is 6 (1), equal to 4 (2), equal to 9 (3).

The calculated equilibrium composition of the mixture of reaction products $SiCl_4$ with H_2 = 6.9, depending on the temperature at a pressure of 550 Torr, is shown in Figure 3. The ratio of the initial components of the $SiCl_4/H_2$ mixture = 6.9 and the pressure were selected based on the experimentally obtained maximum yield of $SiHCl_3$. Figure 3 shows that condensed silicon is created only in the temperature range of 1210–1625 K. The formation of $SiHCl_3$ is observed in the temperature range of 300–2700 K, SiH_2Cl_2 in the range of 750–2500 K, and SiH_3Cl in the range of 1150–1850 K. The formation of $SiCl_2$ and SiHCl radicals is observed in the range of 1000–4500 K and 1230–4300 K, respectively.

Preprints (www.preprints.org) | NOT PEER-REVIEWED | Posted: 9 November 2023 doi:10.20944/preprints202311.0611.v1

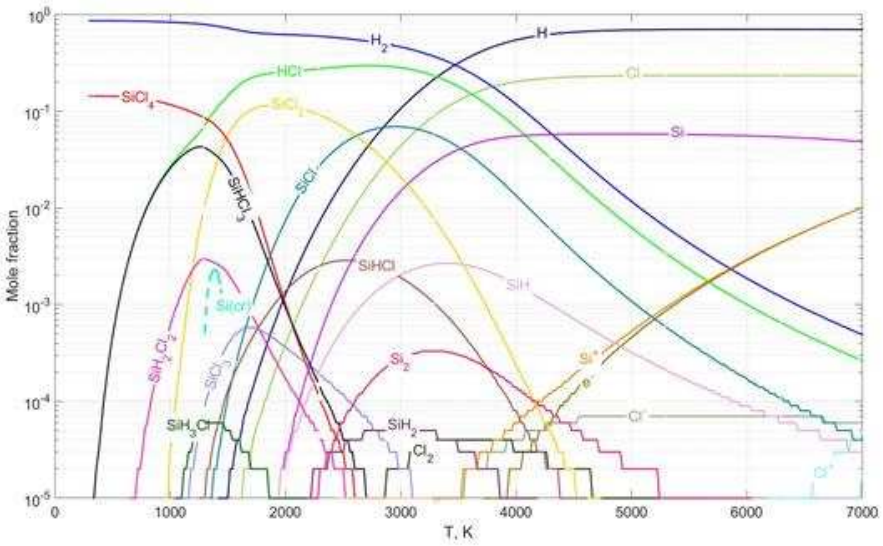

Figure 3. The calculated equilibrium composition of the reaction products as a function of temperature for the ratio $SiCl_4/H_2$ = 6.9, plasma pressure 550 Torr. The dashed line corresponds to the crystalline phase.

In [39,40], it is noted that in the thermodynamic analysis of the Si-H-Cl system, five independent, equilibrium reactions should be taken into account, but in the case of low concentrations of H_2(H_2/$SiCl_4$ 10) and temperatures below 1123–1173K, the number of independent reactions is reduced to two:

$$SiCl_4 + H_2 \rightarrow SiHCl_3 + HCl; \quad (1)$$

$$SiHCl_3 + H_2 \rightarrow Si + 3HCl, \quad (2)$$

as the equilibrium concentrations of SiH_2Cl_2, SiH_3Cl, and $SiCl_2$ become negligible. However, under the discussed conditions, where the influence of active particles formed under plasma conditions, as well as surface phenomena on the electrodes, the formation of dichlorosilane can occur both by the reaction of direct reduction of $SiCl_4$ to SiH_2Cl_2 (3), and by the reaction of dismutation of the formed TCS (4):

$$SiCl_4+2H_2\rightarrow SiH_2Cl_2+2HCl; \quad (3)$$

$$SiHCl_3 + H_2 \rightarrow Si + 3HCl, \quad (4)$$

To clarify the temperature range of the hydrogen reduction of $SiCl_4$, the distribution of thermal and concentration fields in the reaction chamber was determined using CFD modeling. In the full-scale experiment, the zone of plasma formation was a sphere with a radius of ~7 mm, slightly shifted to the upper surface of the reaction chamber, since the outlet of the reacted gas mixture is located at the top (see Figure 1 b). This zone, according to the modeling (Figure 4 a), is in the temperature range of 900–1700 K. The temperature value of 1700 K corresponds to the contact area of the electrode with the plasma. It is in this area, as well as in the area surrounding it, that silicon deposition was observed during the experiment (Figure 5 a). Simultaneously with deposition, the material melted, resulting in a compact sample (Figure 8 a-2). Figure 4 b,c shows an isothermal surface with T = 900 K corresponding to the plasma region and the flow line of the gas mixture through this surface, respectively. According to the conducted numerical experiments, 95% of the gas mixture passes through this surface. Therefore, it can be argued that in the reaction chamber of this configuration, there is almost complete interaction of the gas mixture with the plasma, in which the reactions of reducing silicon tetrachloride to trichloro-, dichlorosilane, as well as silicon take place. The obtained

Preprints (www.preprints.org) | NOT PEER-REVIEWED | Posted: 9 November 2023 doi:10.20944/preprints202311.0611.v1

data on the coefficient of ingress of the gas mixture into the plasma region suggest that the output of TCS equal to 45% is close to the thermodynamic equilibrium at T = 900 K.

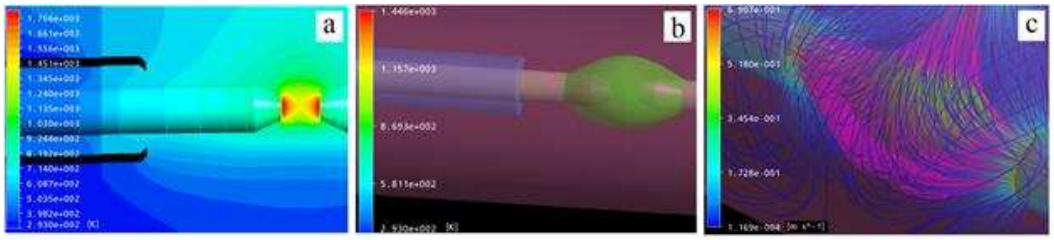

Figure 4. Distribution of the temperature field in the plasma zone, as well as along the length of the electrode (**a**); nozzle system – electrode with an isothermal surface of 900 K (**b**); flow lines of the gas mixture in the nozzle-electrode-isotherm system of 900 K (**c**).

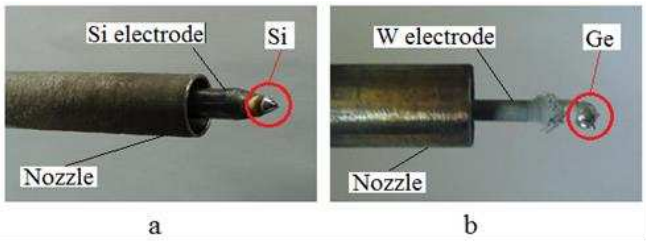

Figure 5. Type of electrodes after hydrogen reduction: $SiCl_4$ (**a**), $GeCl_4$ (**b**).

3.2. Hydrogen reduction of $GeCl_4$

For the process of hydrogen reduction of $GeCl_4$, with an increase in the ratio of reagents $H_2/GeCl_4$ (Figure 6 a) in the initial mixture, the degree of conversion also increases. The main products are $GeHCl_3$ and Ge, formed by the reactions:

$$GeCl_4 + H_2 \rightarrow GeHCl_3 + HCl; \quad (5)$$

$$GeCl_4 + 2H_2 \rightarrow Ge + 4HCl. \quad (6)$$

The dependence of the degree of $GeCl_4$ conversion on the pressure (Figure 6 b) has no maximum. There is a decrease in $GeCl_4$ conversion and Ge yield, and $GeHCl_3$ yield increases. The deposition of Ge on the electrodes is shown in Figure 5. It can be seen that, as in the case of hydrogen reduction of $SiCl_4$, the formation of compact germanium at the ends of the electrodes is observed. It should be noted that Ge is formed not only in the form of an ingot formed at the end of tungsten electrodes but also in the form of fine powder deposited on the inner surface of the reactor.

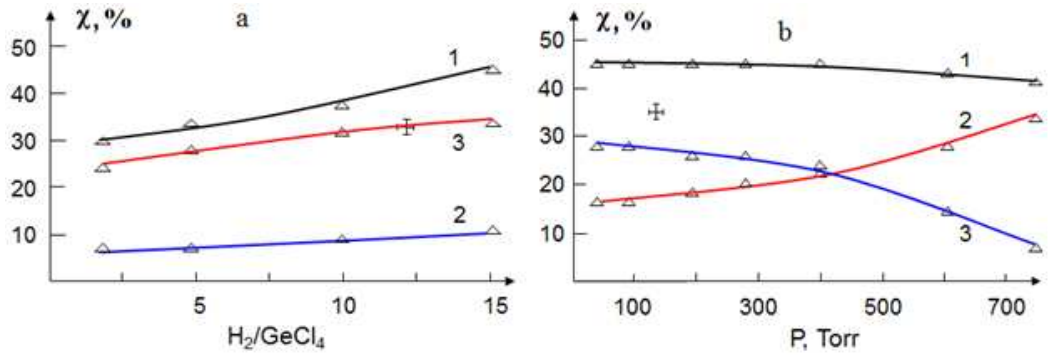

Figure 6. Dependence of the total degree of conversion of $GeCl_4$ (1) and the output of Ge (2) and $GeHCl_3$ (3) on the ratio of $H_2/GeCl_4$ (**a**); dependence of the total degree of conversion of $GeCl_4$ (1) and the output of $GeHCl_3$ (2) and Ge (3) on the pressure in the reactor (**b**).

Preprints (www.preprints.org) | NOT PEER-REVIEWED | Posted: 9 November 2023 doi:10.20944/preprints202311.0611.v1

The calculated equilibrium composition of the products of the interaction of H_2 with $GeCl_4$ depending on temperature at atmospheric pressure is shown in Figure 7. The initial ratio of the content of the components of the mixture $H_2/GeCl_4$ =15 was selected based on the maximum yield of Ge and $GeHCl_3$. Condensed germanium is formed from GTC, in the range of 1250–1500 K. Formation of $GeHCl_3$ compound, according to Figure 7, occurs in the range of 300–1580 K, GeH_2Cl_2 in the range of 500–1580 K, and GeH_3Cl in the range of 760–1500 K.

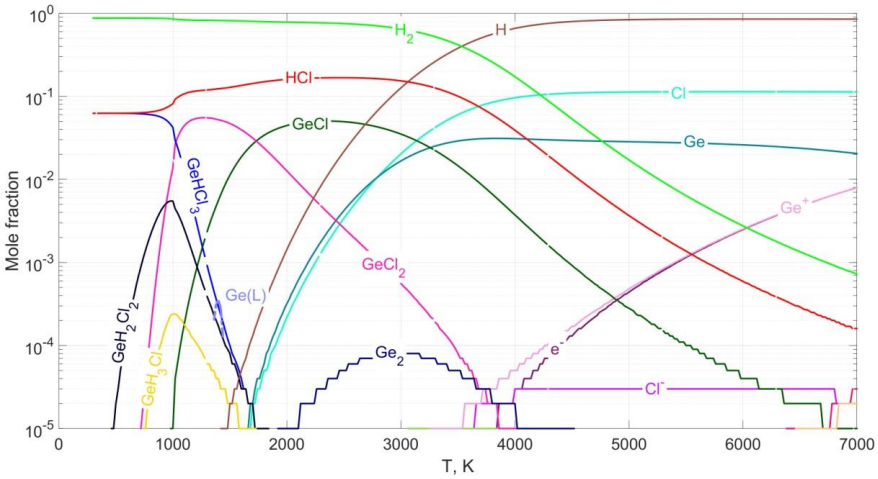

Figure 7. Equilibrium mole fractions of reaction products as a function of temperature for the ratio of $GeCl_4/H_2$ = 15, plasma pressure of 760 Torr.

Based on mathematical modeling, as well as for the process of hydrogen reduction of STC, it was found that in the case of plasma-chemical reduction of GTC in the reaction chamber, almost complete interaction of the gas mixture with plasma also occurred. This makes it possible to assume the equilibrium of the process and estimate the temperature range of the reaction.

According to the experiment, polycrystalline germanium is deposited at the ends of the electrodes, an amorphous germanium powder is formed in the reactor volume, and the analysis of the gas phase confirms the formation of $GeHCl_3$. Equilibrium concentrations shown in Figure 7 also show the possibility of the formation of these substances, which indicates the proximity of the realized experimental conditions to equilibrium. The GeH2Cl2 and GeH_3Cl compounds are not observed experimentally, due to their low equilibrium concentrations.

4. Discussion

4.1. Characterization of samples obtained during the reduction of $SiCl_4$

In the case of hydrogen reduction of $SiCl_4$, the main conversion products are chlorosilanes consisting of a mixture of trichloro- and dichlorosilane, as well as silicon. Table 1 shows the content of metal impurities in the initial $SiCl_4$, as well as a mixture of chlorosilanes and silicon. In addition, the content of electroactive impurities is given for precipitated silicon.

Particular attention was paid to the difficult-to-remove impurities of benzene and hexane, since the concentration of these impurities in STC wastes can reach 1000 ppm.

Preprints (www.preprints.org) | NOT PEER-REVIEWED | Posted: 9 November 2023 doi:10.20944/preprints202311.0611.v1

Table 1. The content of impurities in the initial silicon tetrachloride, the resulting mixture of chlorosilanes and silicon.

Admixture	C, ppm (mol.)		
	Source SiCl4	Chlorosilanes	Si
Fe	0.0100	0.00600	2.60
Cu	0.0005	0.00050	0.04
Cr	0.0020	0.00080	2.20
Mn	0.0040	0.00200	2.20
Ni	0.0002	0.00018	1.30
Mg	0.0100	0.00700	1.60
Al	0.0040	0.00400	≤7.00
B	---	---	≤0.30
P	---	---	≤ 2.00
As	---	---	≤0.30
Sn	---	---	≤0.03
C_6H_6	960	4	---
C_6H_{14}	700	2	---

It can be seen that the content of metal impurities in the mixture of chlorosilanes is at the level of the initial $SiCl_4$, and the concentration of organic substances impurities is reduced by more than two orders of magnitude.

Therefore, in this type of discharge, it is possible to obtain TCS not only with high yield, but also with a significant increase in the purity of both TCS and STC, which is the main requirement for the technology of obtaining high-purity silicon. This possibility appears due to the use of a high-purity silicon electrode as a material. The modes in this case are selected in such a way as to avoid melting the electrode.

Figure 8 shows an image of a silicon electrode before and after silicon deposition.

Figure 8. View of the silicon electrode before (a-1) and after (a-2) carrying out the process of plasma-chemical hydrogen reduction of $SiCl_4$ (**a**); SEM photo of the silicon electrode before (**b**) and after (**c**) carrying out the process of plasma-chemical hydrogen reduction of $SiCl_4$, respectively.

In a silicon sample deposited on the end of the electrode, on the contrary, there is a concentration of metal impurities. Apparently, impurities of metals are in the original $SiCl_4$ in the form of volatile compounds, possibly chlorides, with a binding energy less than that of STC and therefore more easily react with chemically active plasma, which leads to their concentration in the deposited silicon. However, the process of hydrogen reduction of $SiCl_4$ under RF-arc discharge conditions can be used to obtain high-purity monocrystalline samples, subject to mandatory post-treatment of polysilicon by zone recrystallization or Czochralski monocrystal growth, since the concentration of electroactive impurities Al, B, P, As, and Sn in silicon is below the detection limit.

4.2. Samples of germanium obtained in RF-arc discharge from $GeCl_4$

Preprints (www.preprints.org) | NOT PEER-REVIEWED | Posted: 9 November 2023 doi:10.20944/preprints202311.0611.v1

Experimentally, it was shown that under the conditions of RF-arc discharge at a pressure below atmospheric pressure, from a mixture of $GeCl_4$ + H_2, at the ends of the electrodes, compact Ge is formed. In addition, Ge is also formed as a powder deposited on the inner surface of the reactor. The compact Ge, according to X-ray phase analysis, is polycrystalline. Table 2 shows the impurity composition of the initial $GeCl_4$ and the resulting compact Ge.

Table 2. Impurity composition (ppm wt) of the initial $GeCl_4$ and compact Ge.

Admixture	Source $GeCl_4$	Ge	Admixture	Source $GeCl_4$	Ge
B	0.300	0.300	**Co**	0.002	0.003
Al	<1.900	<1.900	**Fe**	0.030	8.100
P	1.200	1.200	**Cu**	<0.200	<0.200
As	0.500	0.500	**Zn**	<0.100	<0.100
Sb	0.003	0.003	**Cr**	0.800	0.700
Sn	0.100	0.100	**Mn**	0.010	0.010
W	0.100	170,000	**Mo**	0.800	0.600
Ti	<0.200	<0.200	**Mg**	<0.400	<0.400

It can be seen that the content of impurities in Ge is at the level of purity of the original $GeCl_4$. Exceptions are impurities W and Fe coming from structural materials (tungsten electrode and stainless-steel nozzles). However, these impurities can easily be removed by zone recrystallization or the Czochralski method [41].

Of particular interest is also the powdered Ge. Nanocrystals of germanium can be of interest for various electronic and optoelectronic applications, primarily due to the possibility of adjusting the bandwidth from the infrared to the visible range of the spectrum depending on the size [26,27].

Figure 9 a-d shows the TEM image of this sample.

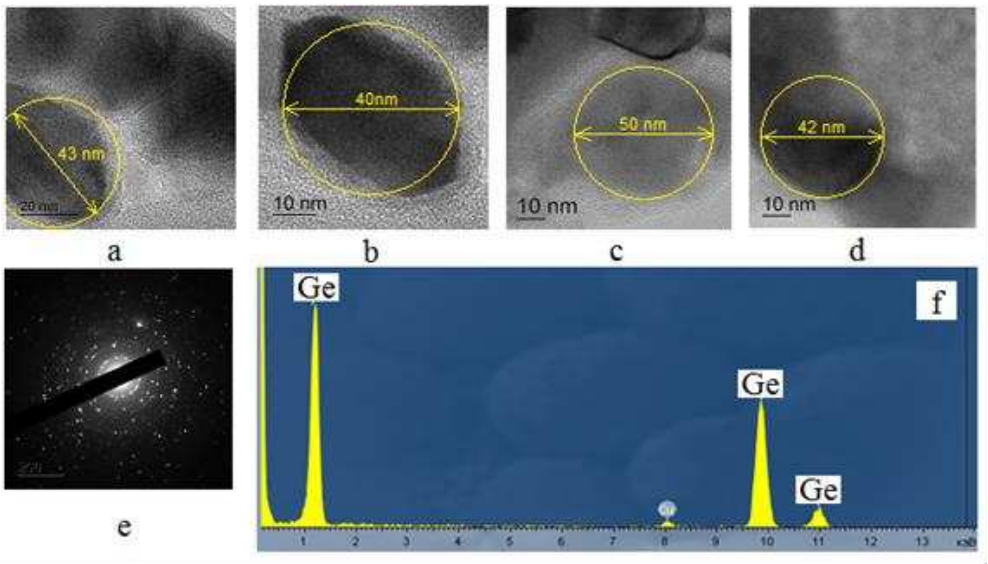

Figure 9. TEM image of Ge nanoparticles (**a**-**d**); diffraction pattern of Ge nanoparticles (**e**); spectrum of characteristic X-ray lines (**f**).

The powdered Ge is a nanoparticle. The diffraction pattern of the sample (Figure 9 e) indicates that these particles are monocrystalline, and according to X-ray microanalysis (Figure 9 f), the Ge sample obtained does not contain Cl and O impurities.

 doi:10.20944/preprints202311.0611.v1

In the study of nanostructured germanium samples by laser diffraction using dispersion, it was impossible to carry out a complete separation of agglomerates, which did not make it possible to correctly estimate the particle size distribution. Therefore, the evaluation of this parameter was carried out on the basis of photographs obtained by TEM. Particle sizes have been shown to range from 22 to 75 nm with an average size of 40–50 nm. Thus, in the RF-arc discharge, in the pressure range of 30–760 Torr, conditions are created for obtaining not only compact Ge but also Ge in the form of nanoparticles.

5. Conclusions

Based on the studies conducted, it was established that the RF-arc discharge could be used to obtain high-purity chlorosilanes and silicon from STC wastes. The content of the target products in the experimental conditions is close to equilibrium, which is confirmed by thermodynamic analysis. By numerical gas-dynamic modeling of thermal and concentration fields, zones in the plasma-chemical reactor were established, in which the values of product concentrations correspond to equilibrium ones. It has been established that the proposed reactor design makes it possible to carry out the reaction of reduction of STC and GTC with hydrogen under conditions close to equilibrium.

It has been established that the RF-arc discharge can be used for the synthesis of trichlorogermane or TCS from GTC or STC, as well as for the production of semiconductor germanium or silicon in the form of polycrystalline ingots, and germanium also in the form of nanopowder with an average particle size of 40–50 nm.

Author Contributions: Conceptualization, R.K. and G.M.; methodology, R.K., I.G., A.K.; validation, N.R., S.R.; resources, I.G., L.S., A.K., N.R., S.R., V.A., ,D.B. and N.M.; writing—review and editing, R.K.; visualization, G.M., N.M. and N.K.; supervision, G.M.; project administration, R.K. and G.M. All authors have read and agreed to the published version of the manuscript.

Funding: The study was carried out within the framework of the state task in the field of scientific activity (topic No. FSWE-2022-0008).

Data Availability Statement: Data used in this study are available from the corresponding author.

Conflicts of Interest: The authors declare no conflict of interest.

References

1. Zulehner, W. Historical overview of silicon crystal pulling development. *Mater. Sci. Eng. B* **2000**, *73*, 7–15.
2. McHugo, S.A., Thompson, A.C., Mohammed, A., Lamble, G., Périchaud, I., Martinuzzi, S., Werner, M., Rinio, M., Koch, W., Hoefs, H.U., Haessler, C. Nanometer-scale metal precipitates in multicrystalline silicon solar cells. *J. Appl. Phys.* **2001**, *89*, 4282–4288.
3. Zhang, X., Gong, L., Wu, B., Zhou, M., Dai, B. Characteristics and value enhancement of cast silicon ingots. *Sol. Energy Mater Sol. Cells* **2015**, *139*, 27–33.
4. Cariou, R., Tang, J., Ramay, N., Ruggeri, R., Roca i Cabarrocas, P. Low temperature epitaxial growth of SiGe absorber for thin film heterojunction solar cells. *Sol. Energy Mater Sol. Cells* **2015**, *134*, 15–21.
5. Leal, R., Dornstetter, J.C., Haddad, F., Poulain, G., Maurice, J.L., Roca i Cabarrocas, P. Silicon epitaxy by low-temperature RF-PECVD using SiF4/H2/Ar gas mixtures for emitter formation in crystalline solar cells. In 42nd Photovoltaic Specialist Conference (PVSC), New Orleans (2015).
6. Kim, W., Matsuhara, H., Onaka, T. et al. Optical performance evaluation of near-infrared camera (NIR) on board ASTRO-F. In Cryogenic Optical Systems and Instruments XI,5904, 590418 (2005).
7. Fonollosa, J., Rubio, R., Hartwig, S., Marco, S., Santander, J., Fonseca, L., Wollenstein, J., Moreno, M. Design and fabrication of silicon-based mid infrared multi-lenses for gas sensing applications. *Sens. Actuators B Chem.* **2008**, *132*, 498–507.
8. Houssa, M. *Germanium-Based Technologies: From Materials to Devices*; Oxford: Elsevier, 2007.
9. Raudorf, T.W., Trammel, R.C., Darken, L.S. N-type high purity germanium coaxial detectors. *IEEE Trans. on Nucl. Sci.* **1979**, *26*, 297–302.
10. Pehl, R.H., Madden, N.W., Elliott, J.H. Radiation damage resistance of reverse electrode Ge coaxial detectors. *IEEE Trans. on Nucl. Sci.* **1979**, *26*, 321–323.
11. Eaglesham, D.J., Cerullo, M. Dislocation-free Stranski-Krastanow growth of Ge on Si(100). *Phys. Rev. Lett.* **1990**, *64*, 1943–1947.
12. Chu, S., Majumdar, A. Opportunities and challenges for a sustainable energy future. *Nature* **2012**, *488*, 294–303.

13. Bathey, B.R., Cretella, M.C. Solar-grade silicon. *J. Mater. Sci.* **2005**, *17*, 3877–3896.
14. Vorotyntsev, A., Markov, A., Petukhov, A., Atlaskina, M., Atlaskin, A., Kapinos, A., Vorotyntsev, V., Pryakhina, V. Catalytic disproportionation of chlorosilanes using imidazolium ionic liquids supported on polymer supports. *Catal. Ind.* **2021**, *13*, 1–11.
15. Matveev, A.K., Mochalov, G.M., Suvorov, S.S. Method of Obtaining Silane and Chlorosilanes. RU Patent No. 2608523, 2015.
16. Jarkin, V.N., Kisarin, O.A., Kritskaya, T.V. Methods of trichlorosilane synthesis for polycrystalline silicon production. *Izv. Vuzov. Mat. Elec. Tech.* **2021**, *24*, 5–26.
17. Bolshakov, K.A. *Chemistry and Technology of Rare and Scattered Elements*, Part 2; Vysshaia shkola: Moscow, 1976; pp. 192–196.
18. Wu, L., Ma, Zh., He, A., Wang, J. Decomposition of silicon tetrachloride by microwave plasma jet at atmospheric pressure. *Inorg. Mater.* **2009**, *45*, 1403–1407.
19. Wu, L., Ma, Zh., He, A., Wang, J. Studies on destruction of silicon tetrachloride using microwave plasma jet. *J. Hazard. Mater.* **2010**, *173*, 305–309.
20. Lu, Zh., Zhang, W. Hydrogenation of silicon tetrachloride in microwave plasma. *Chin. J. Chem. Eng.* **2014**, *22*, 227–233.
21. Wu, Q., Chen, H., Li, Y., Tao, X., Huang, Zh., Shang, Sh., Yin, Y., Dai, X. Preparation of trichlorosilane from hydrogenation of silicon tetrachloride in thermal plasma. *Inorg. Mater.* **2010**, *46*, 251–254.
22. Gromov, G.N., Bolgov, M.V., Muravitski, S.A. Method for Obtaining Trichlorosilane by Plasma-Chemical Hydrogenation of Silicon Tetrachloride and a Device for its Implementation. Patent RF (RU) No. 2350558, 685, 2009.
23. Sarma, K.R., Rice, M.J. High Pressure Plasma Hydrogenation of Silicon Tetrachloride. US Patent No. 4, 309, 259, 1982.
24. Fang, Y.Z., Ma, W.Y., Zhou, J.H., Lu, C., Wu, J.G. Theoretical study on the reaction mechanism of $GeHCl_3$ + $CH_2CHCOOH$ → $GeCl_3CH_2CH_2COOH$. *J. Mol. Struct.: THEOCHEM* **2008**, *857*, 51–56.
25. Menchikov, L.G., Ignatenko, M.A. Biological activity of organogermanium compounds (a review). *Pharm. Chem. J.* **2013**, *46*, 635–638.
26. Gielen, M., Tiekink, E.R.T. *Metallotherapeutic Drugs and Metal-Based Diagnostic Agents. The use of Metals in Medicine*; Wiley, 2005.
27. Ahadi, A.M., Hunter, K.I., Kramer, N.J., Strunskus, T., Kersten, H., Faupel, F., Kortshagen, U.R. Controlled synthesis of germanium nanoparticles by nonthermal plasmas. *Appl. Phys. Lett.* **2016**, *108*, 093105.
28. Gresback, R., Holman, Z., Kortshagen, U. Nonthermal plasma synthesis of size-controlled, monodisperse, freestanding germanium nanocrystals. *Appl. Phys. Lett.* **2007**, *91*, 093119.
29. Whitham, P.J., Strommen, D.P., Lundell, S., Lau, L.D., Rodriguez, R. GeS_2 and $GeSe_2$ PECVD from GeCl4 and Various Chalcogenide Precursors. *Plasma Chem. Plasma Process* **2014**, *34*, 755–766.
30. Lang, J.E., Rauleder, H., Muh, E. Method for Producing Higher Silanes with Improved Yield. WO Patent No. 007426 A1, 2013.
31. Gribov, L.A., Smirnov, V.N. Intensities in the infrared absorption spectra of polyatomic molecules. *Usp. Fiz. Nauk* **1961**, *527*, 527–567.
32. CEARUN. Available online: https://cearun.grc.nasa.gov (accessed on 15 April 2020)
33. Smith, W.R., Missen, R.W. *Chemical Reaction Equilibrium Analysis: Theory and Experiment*; Wiley: New York, 1982.
34. Shabanov, S.V., Gornushkin, I.B. Two-dimensional axisymmetric models of laser induced plasmas relevant to laser induced breakdown spectroscopy. *Spectrochim. Acta B* **2014**, *100*, 147–172.
35. Belov, G.V., Iorish, V.S., Yungman, V.S. Simulation of equilibrium states of thermodynamic systems using IVTANTERMO for Windows. *High Temp.* **2000**, *38*, 191–196.
36. Shabarova, L.V., Plekhovich, A.D., Kutyin, A.M., Sennikov, P.G., Kornev, R.A. Modeling thermogasdynamic processes in the production of silicon from its halides. *Theor. Found. Chem. Eng.* **2020**, *54*, 504–513. https://doi.org/10.31857/S0040357120040144
37. Murphy, A.B. Transport coefficients of hydrogen and argon–hydrogen plasmas. *Plasma Chem. Plasma Process.* **2000**, *20*, 279–297. https://doi.org/10.1023/A:1007099926249
38. Furman, A.A. *Inorganic Chlorides*; Khimiya: Moscow, 1980.
39. Nigmatulin, R.I. *Dynamics of Multiphase Media*. Part 1; Nauka: Moscow, 1987.
40. Chanley, C.S. Patent 4542004 USA.
41. Wolf, W.E., Teichmann, R. Zur Thermodynamik des Systems Si-Cl-H. Z. *Anorg. Allg. Chem*. **1980**, *460*, 65–80.